X-811-72-470

PREPRINT

NASA TM X- 66154

COMPUTER CONTROLLED ANTENNA SYSTEM

NICHOLAS A. RAUMANN

DECEMBER 1972

GSFC — GODDARD SPACE FLIGHT CENTER
GREENBELT, MARYLAND

X-811-72-470

COMPUTER CONTROLLED ANTENNA SYSTEM

Nicholas A. Raumann

December 1972

Goddard Space Flight Center
Greenbelt, Maryland

ACKNOWLEDGMENT

The author is deeply indebted to Mr. G. C. Winston of the Laser Data Systems Branch for the encouragement and technical assistance and advice received. The author would also like to acknowledge the contributions of Mr. J. F. Vinson of the Antenna Systems Branch in implementing and evaluating the various programs. Likewise acknowledgment is due to Dr. J. Zarur and Mr. B. Baymler of Wolf Research and Development Corporation for programming support.

COMPUTER CONTROLLED ANTENNA SYSTEM

Nicholas A. Raumann

ABSTRACT

With the advent of relatively cheap and small computers on the market, digital techniques become a very attractive application to the servo and control system of large antennas. A small dedicated digital computer can be used economically to replace certain pieces of existing hardware and can be used, in addition, to perform an automatic checkout and readiness verification of the servo system. Such a system has several advantages: reliability and consistency of operation, minimization of turn around time between satellite passes and fast identification of component or subsystem failures or misadjustments.

These techniques have been evaluated at the Network Test and Training Facility (NTTF) using the 40-foot antenna and the Sigma V computer. Programs have been completed which drive the antenna directly without the need for a servo amplifier, antenna position programmer or a scan generator. In addition, several programs have been developed which test the operation of the servo system and diagnose subsystem failure or misadjustments.

CONTENTS

COMPUTER CONTROLLED ANTENNA SYSTEM

1. INTRODUCTION

With the advent of relatively cheap and small computers on the market, digital techniques become a very attractive application to the servo and control system of large antennas. A small dedicated computer can be used to perform automatic checkout and readiness verification of the servo system. In addition, the computer can be used to replace certain pieces of existing hardware. The tracking performance of the antenna can also be improved by use of improved control algorithms.

These techniques have been evaluated at Goddard's Network Test and Training Facility using the 40-foot data acquisition antenna and an XDS/Sigma V computer. Even though this computer is a much larger machine than is necessary for this application, the feasibility of the various techniques has been established. All real time programs have been written in assembly language (SYMBOL), while most test programs have been written in FORTRAN IV for reasons of expediency. Programs have been evaluated under realistic conditions and system operation has been demonstrated by tracking NIMBUS and OGO satellites.

Software developed in support of the monitoring and automatic checkout function is shown in Figure 1.1. During normal operation of the antenna system the computer monitors critical quantities such as power supplies, oil temperatures, axis velocities and limits. Abnormal conditions are flagged to the operator and if condition warrants it, direct action is taken by the computer. The antenna operator can call for an initialization program, which automatically brings the antenna to operational status by properly sequencing the various switching functions.

A readiness verification program can be called which is intended as a short prepass check of the servo system. This program checks power supplies, circuit breakers, interlocks, and the hydraulic system. As a final test a step function is applied to the antenna and its transient response is evaluated according to a predetermined performance index. If all of these tests pass satisfactorily, the antenna is declared operational. If not, the operator is informed of the particular problem and is given the choice of operating the antenna in a degraded mode or calling the complete diagnostic test program which will help in further pinpointing the problem.

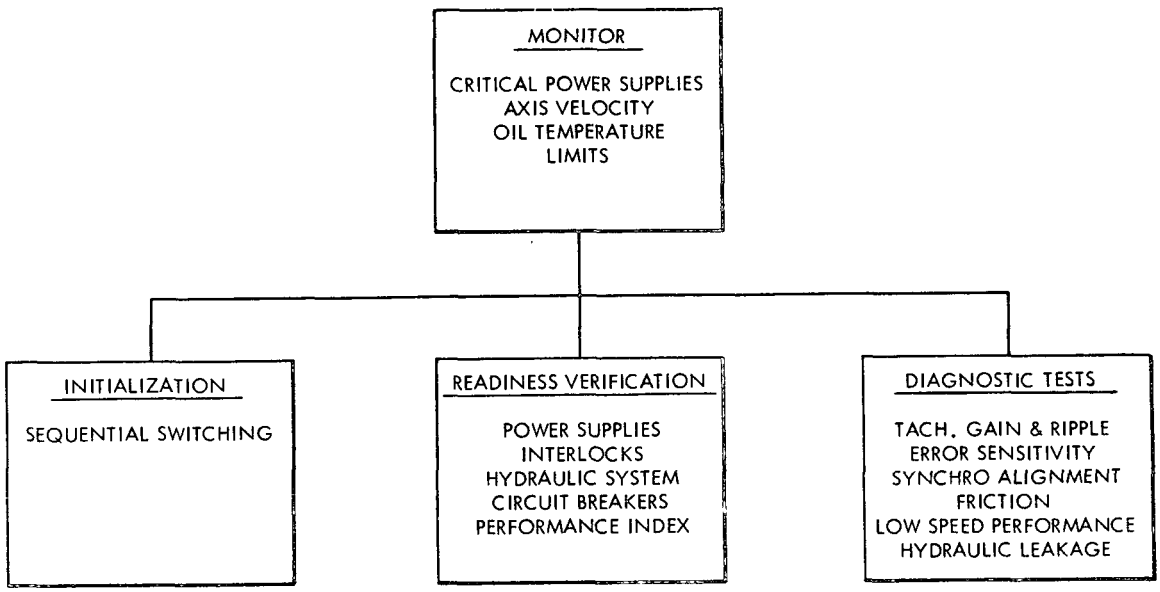

Figure 1-1. Programs for Monitoring and Automatic Checkout of Antenna.

The diagnostic test program checks for items such as tachometer gain and ripple, error sensitivity, synchro operation, friction, low speed performance, and hydraulic leakage; and finally generates a diagnostic message to the operator. This program can also be called during the performance of routine maintenance, because many tests of this program coincide with tests required by standard maintenance procedures.

Figure 1-2 shows the tracking loop for an antenna as it exists at a typical STDN tracking site. The antenna structure is driven by a hydraulic drive system, while the tachometer, receiver and encoder provide feedback signals from the structure. The tracking loop is closed via the servo amplifier and the receiver or the antenna position programmer depending on the operating mode selected. Off-line the PB 250 computer (UNIVAC 1218 for USB antennas) is used to generate predict data and a scan generator is provided which aids during the satellite acquisition phase.

All devices shown crosshatched in Figure 1.2 are special purpose equipment ranging in size from one chassis to several racks. The function of these devices have been replaced with a program on the same computer. Test results indicate that the digital system has a performance that is equal to or better than the performance of the existing system.

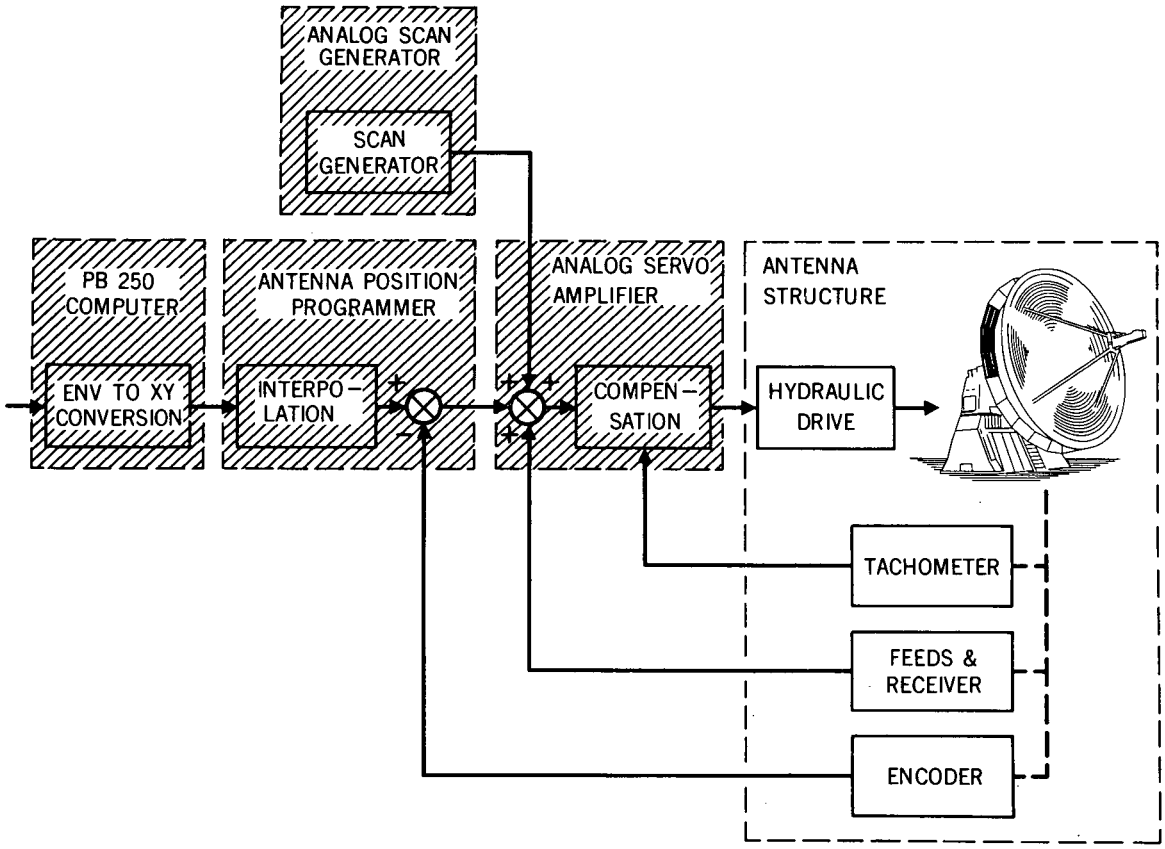

Figure 1-2. Tracking Loop of Antenna.

Using the computer approach, the tracking performance of the antenna can be improved. This has been accomplished by addition of a new mode of operation, termed "augmentation mode." This mode permits operation in the program mode with the addition of a correction factor derived from the receiver and passing it through a low-pass filter and integrator. Thus, the antenna is driven by a signal with high signal-to-noise ratio, as it would normally be during program mode operation but improved pointing capability is provided by the introduction of the average receiver output.

Conceptually, this project has been outlined in reference 1.1.

2. MONITORING AND AUTOMATIC CHECKOUT

The Monitor, Initialization, Readiness Verification and Diagnostic Test programs identified in Figure 1.1 consist of a calling sequence of various subroutines which test or measure certain aspects of the antenna aystem. These programs form the link between the computer, the antenna system and the operator and since they consist of logical manipulations of subroutines they will not be discussed in detail. The discussions below will concentrate on techniques employed in the various subroutines and is largely based on a study covered in reference 2.1. In these discussions reference is made to various operating modes of the antenna and figure 2.1 is included to show the implementation of these modes in the antenna system.

2.1 AC Power

In this application various amplitudes have to be measured at a nominal frequency of 60 Hz. Amplitude is determined by taking 300 samples at a 12 KHz rate. From these samples, 200 consecutive samples are chosen, such that the first sample has a magnitude of 10% or less of the absolute peak value. If such a sample complement cannot be found, all 300 samples are rejected, and a new sampling process is initiated. This procedure insures that the measurement accuracy will be below a certain value and at the same time the sampling process will take less than 25 ms.

The root-mean-square (rms) value of the voltage rms is then determined by using:

$$V_{rms} = \left[\frac{1}{200} \sum_{K=1}^{200} E_K^2 \right]^{1/2}$$

where E_k = voltage sampled at k-th interval, volts

The accuracy of this measurement including the analog-to-digital converter accuracy is ±0.1%.

The frequency is established by scanning the 300 samples and determining the number of samples, N, from polarity change tc polarity change of the same sense. Frequency f in Hz is then computed using

$$f = \frac{12000}{N}$$

The accuracy of this measurement is ±0.5%.

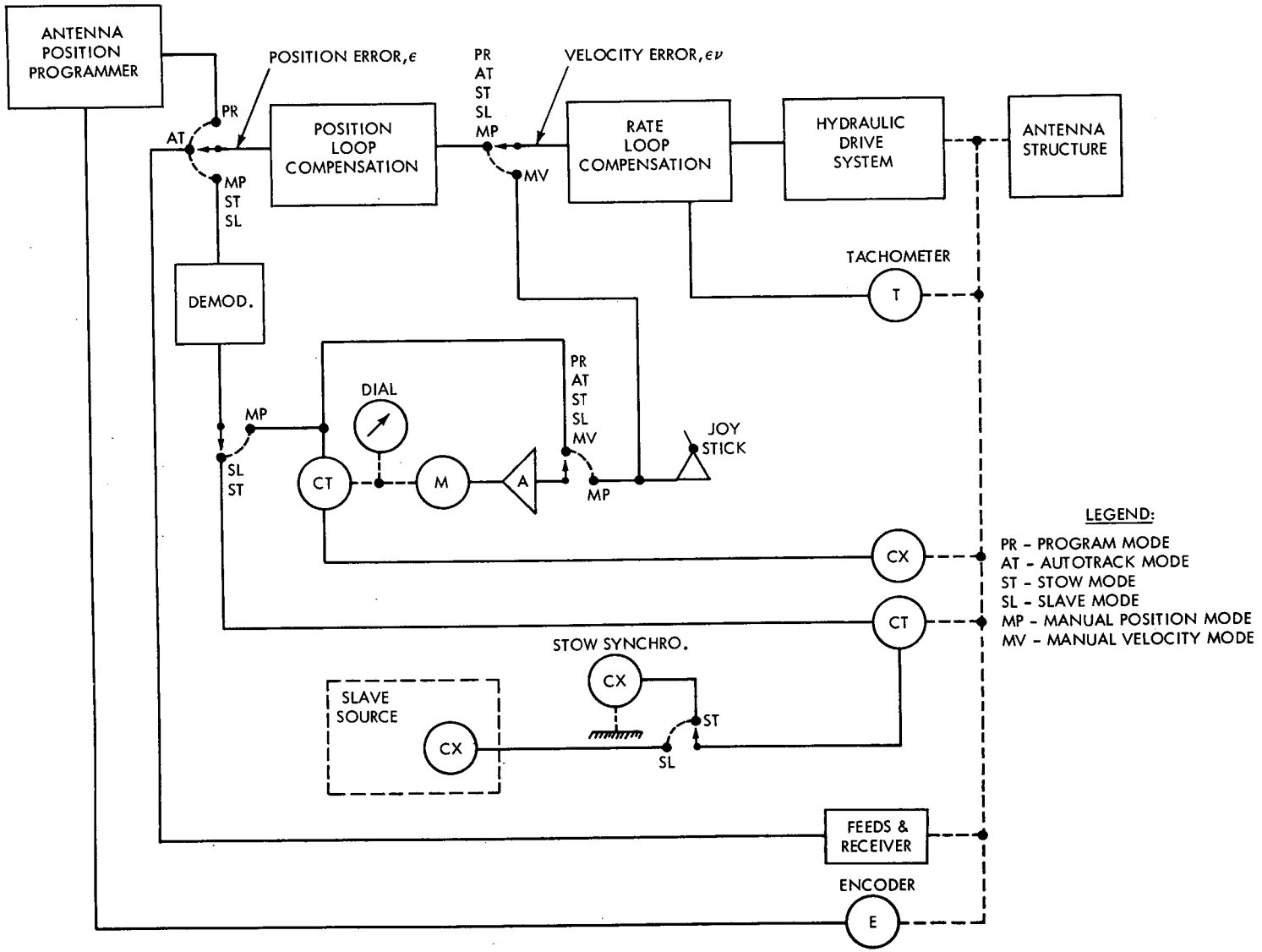

Figure 2-1. Simplified Diagram of the Control and Drive System

2.2 DC Power and Hydraulic Pressure

DC voltage levels are measured by taking 200 samples at 12 KHz rate. The average value of the voltage, V_{ave}, is computed by

$$V_{ave} = \frac{1}{200}\sum_{K=1}^{200} E_k \tag{2.1}$$

This measurement is accurate to ±0.1%.

Ripple, V_{rms}, riding on this dc voltage is established using:

$$V_{rms} = \left[\frac{1}{200}\sum_{k=1}^{200}(E_k - V_{ave})^2\right]^{1/2} \tag{2.2}$$

This measurement is accurate to ±2%.

Hydraulic pressure is measured by means of pressure transducers whose output is a dc voltage proportional to pressure. Hence, measurement involves determination of V_{ave} and V_{rms} using equations (2.1) and (2.2), and applying an appropriate conversion factor.

2.3 Tachometer Gain and Ripple

In this test a constant voltage is applied to the rate loop of the antenna. After the decay of transients, tachometer output and encoder are sampled at a 100 Hz rate until 500 sample pairs have been collected. The average and rms tachometer voltages are computed using relationships (2.1) and (2.2) only changing the summation limit to 500. Antenna velocity, $\dot{\theta}_{ave}$, is established from the encoder readings:

$$\dot{\theta}_{ave} = \frac{1}{1250}\sum_{K=1}^{500}(\theta_K - \theta_0) \tag{2.3}$$

where θ_K = encoder reading at k'th interval.

θ_0 = initial encoder reading.

From this tachometer gain is computed:

$$\text{Gain} = \frac{V_{ave}}{\dot{\theta}_{ave}}$$

Ripple is computed by establishing first the velocity ripple, $\dot{\theta}_{rms}$, of the antenna as measured by the encoder and then forming the difference in root-mean-square fashion between rms tachometer voltage and $\dot{\theta}_{rms}$:

$$\dot{\theta}_{rms} = \left[\frac{1}{1250}\sum_{K=1}^{500}\left(\theta_K - \theta_0 - \frac{k}{250}\dot{\theta}_{ave}\right)^2\right]^{1/2}$$

$$\text{Ripple} = \left[\left(\frac{V_{rms}}{\text{gain}}\right)^2 - \dot{\theta}^2_{rms}\right]^{1/2} \tag{2.4}$$

2.4 Low Rate Performance

This test is used to establish whether the antenna can operate smoothly at a low velocity and is performed for the rate loop and then repeated for the position loop. A constant velocity input is provided for either loop and after decay of transients, 500 encoder samples are taken at a 100 Hz rate. Velocity and ripple are computed using relationships (2.3) and (2.4).

2.5 Deceleration Test

This test is performed to assure that maximum antenna deceleration is within certain limits and that the antenna comes to a complete stop within a specified time. The antenna is moved at a constant velocity and the brakes are applied. Prior to application of brakes 500 encoder and 500 tachometer samples are taken to a 100 Hz rate. From this the average velocity $\dot{\theta}_{ave}$ and the average tachometer voltage V_{ave} are computed using equations 2.3 and 2.1 respectively. After the application of the brakes 1000 tachometer voltage samples are taken at a 800 Hz rate. Deceleration, $\ddot{\theta}$, is computed by means of the following expression:

$$\ddot{\theta} = \frac{1600}{(K_b - K_a)^2} \frac{\dot{\theta}_{ave}}{V_{ave}} \sum_{K=Ka}^{K_b} (V_k - V_a)$$

where K_a = 1st sample at which $V_k \leq 0.9\ V_{ave}$

K_b = 1st sample at which $V_k \leq 0.1\ V_{ave}$

After establishment of $\ddot{\theta}$, the remaining tachometer voltage samples are scanned and the total stopping time is determined.

2.6 Breakaway Torque

This test measures the breakaway torque and hence, the amount of static friction encountered in the antenna system. A step function of sufficient magnitude is applied to the rate loop., 500 samples pairs are taken of the differential pressure, P, across the hydraulic motors and of the encoder at a rate of 100 Hz. The sample, K_b, is determined at which the encoder changes value. Thus the breakaway torque, T, is computed:

$$T = \frac{2\ k_m}{k_b} \sum_{K=0}^{K_b} P_k$$

where K_m = motor torque constant.

2.7 Error Sensitivity

This test is used to establish the error sensitivities in the various positional modes of operation of the antenna. A particular mode is selected and the antenna is permitted to null out. Then 200 initial sample pairs are taken of the error voltage, ϵ, and encoder output at a rate of 100 Hz. The initial averages are computed for the error voltage, $\epsilon_{i\ ave}$, and encoder, $\theta_{i\ ave}$, using equation (2.1). Then an offset voltage of approximately 1 degree is introduced. After transients have died away another 200 sample pairs are taken and final values for error voltage, $\epsilon_{f\ ave}$, and encoder $\theta_{f\ ave}$ are computed. The error sensitivity, S, is then established:

$$S = \frac{\epsilon_{f\ ave} - \epsilon_{i\ ave}}{\theta_{f\ ave} - \theta_{i\ ave}} \tag{2.5}$$

The amount of noise on the error signal is then calculated using equation (2.2) to find $\epsilon_{i\ rms}$ and $\epsilon_{f\ rms}$. The total noise is then defined as:

$$\text{Noise} = \frac{1}{2}\left[\epsilon^2_{i\ rms} + \epsilon^2_{f\ rms}\right]^{1/2}$$

The above procedure is repeated for all positional modes.

2.8 Synchro Alignment

Synchros are used in the manual position, slave and stow modes. The alignment of these synchros is checked by entering the various modes and reading the encoders and error voltages after transients have disappeared. 200 sample pairs are taken at a 100 Hz rate and the average encoder reading, θ_{ave}, and the average error voltage, ϵ_{ave}, are determined using equation (2.1). The synchro alignment, θ_s, is then found:

$$\theta_s = \theta_{ave} + S\,\epsilon_{ave}$$

where the error sensitivity, S, has been established in equation (2.5).

2.9 Hydraulic Drive System

The schematic of the hydraulic drive system is shown in Figure 2.2 (Only one axis drive is shown.) In this test the antenna is operated at a constant speed of 4°/sec and then 1°/sec. For both speeds pressures P_1, P_2, P_3, P_4 and P_5; differential pressures ΔP_1 and ΔP_2; flow rates Q_1 and Q_2; and valve current I_v are measured. Measurement follows the procedure discussed in Section 2.2.

First, the filter constants K_{f1} and K_{f2} are computed which represent the degree to which the filters are clogged (using 4°/sec data):

$$K_{f1} = \frac{\Delta P_1}{Q_1^2} \quad \text{and} \quad K_{f2} = \frac{\Delta P_2}{Q_2^2}$$

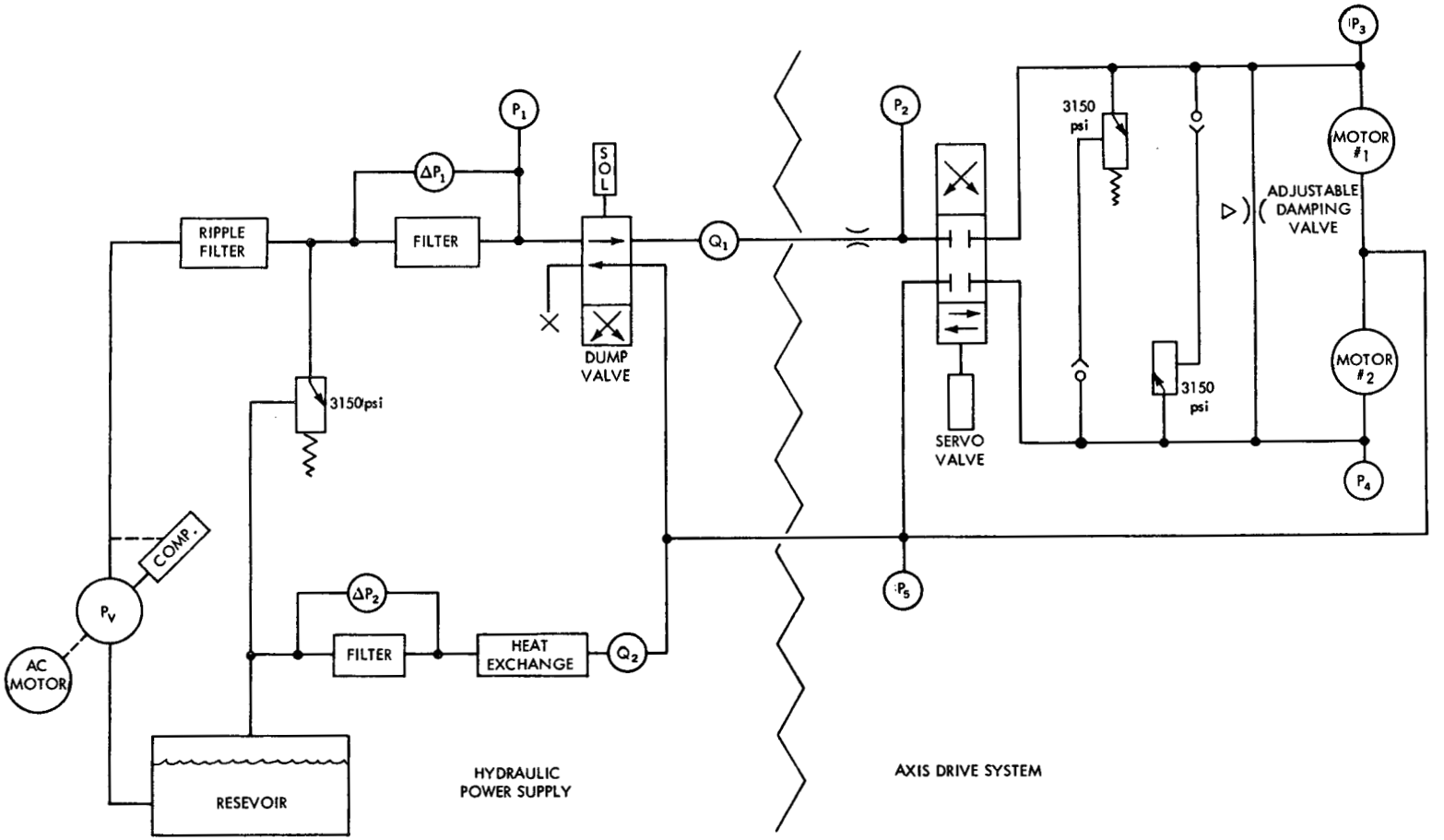

Figure 2-2. Hydraulic Drive System

Then the line drops K_{e1} and K_{e2} are established (using 4°/sec data):

$$K_{e1} = \frac{P_1 - P_2}{Q_1^2} \quad \text{and} \quad K_{e2} = \frac{P_5 - \Delta P_2}{Q_2^2}$$

Subsequently, drive system leakage is computed by using the following equation

$$Q_1 = L_m P_3 + L_d (P_3 - P_4) + D_m \dot{\theta}_m$$

where

L_m = internal motor leakage

L_d = leakage through damping valve

D_m = displacement constant of hydraulic motor

$\dot{\theta}_m$ = motor shaft velocity

By substituting values into above equation corresponding to antenna speed of 4°/sec and then 1°/sec, the two unknowns L_m and L_d can be numerically evaluated.

Finally, the gain of the servo valve, K_s, and the gain of the hydraulic drive system, K_h, are established:

$$K_s = \frac{Q_1}{I_v \sqrt{P_2 - P_3}}$$

and

$$K_h = \frac{\dot{\theta}_m}{I_v}$$

Equations in this section have assumed that motor number one is driving or $P_3 > P_4$. Equivalent analysis can be performed on motor number two.

2.10 Rate Loop Performance Index

The rate loop performance index is a measure of the transient response of the rate loop; a lower number of the index indicating a better performance. The

test is performed by applying a step function to the rate loop and sampling the velocity error, ϵ_ν, at a rate of 100 Hz until 500 samples have been collected. The rate loop performance index, RPI, is computed using a formula that was empirically developed:

$$RPI = \frac{RT}{0.07} + 10\,\frac{\epsilon_{\nu\ rms}}{\epsilon_{\nu\ ave}};\quad RT \geq 0.07$$

where

RT = rise time, s

$\epsilon_{\nu\ rms}$, $\epsilon_{\nu\ ave}$ = steady state ripple and average velocity error respectively using last 300 samples.

The characteristics of such a performance index can be judged from Figure 2.3 where the index is plotted vs. loop gain. Also shown in that figure are step function responses for low, nominal and high loop gain.

2.11 Position Loop Performance Index

This performance index is essentially similar to the previous one except that the transient response of the position loop is evaluated. 1000 samples of the position error are taken at a 100 Hz rate. These samples are taken for both type I and type II operation of the position loop. (Type II operation corresponds to a loop having an additional integration, whereas type I does not have this integration.) Empirically the position loop performance index for type I operation, PPI_1, has been established as:

$$PPI_1 = \frac{1}{0.75}\left(\frac{OS}{8} + ST\right);\quad ST \geq 0.75$$

where

OS = overshoot, percent

ST = settling time, seconds
(= elapsed time up to a point after which response stays within 5% of final value.)

The index for type II operation, PPI_2, is:

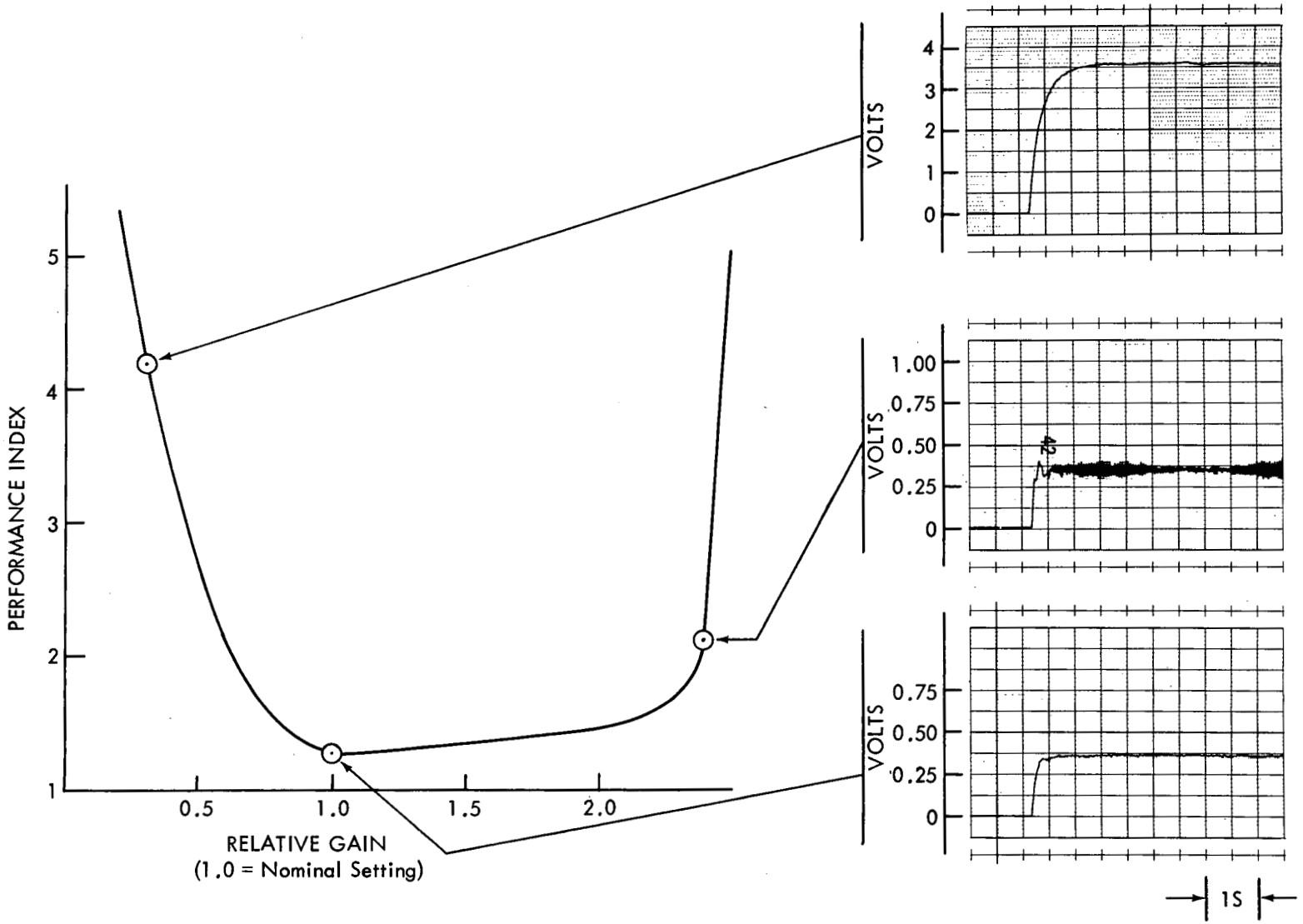

Figure 2-3. Performance Index for Rate Loop

$$PPI_2 = \frac{1}{3.5}\left(3\frac{OS}{40} + \frac{ST}{3}\right), \quad OS \geq 40, \quad ST \geq 1.5$$

Graphically the characteristics of these indices are shown in Figures 2.4 and 2.5.

It should be noted here that experimentation has been done with more conventional indices such as ISE (integral of the square error), ITAE (integral of product of time and absolute error) and several others. However, all of these indices showed a lack of sensitivity around the nominal setting.

3. TRACKING LOOP

As was pointed out in the introduction the tracking loop can be closed via the computer replacing several pieces of special purpose hardware. In this project an attempt has been made to replace hardware functions on a one-to-one basis, i.e. no improvements or optimizations of the tracking loop have been attempted. However, it should be stressed, that if improvements or changes are required, the computer approach yields a high degree of flexibility.

The antenna system, as it exists in the field today, is operated from a control console which is an arrangement of several racks. The operator is provided with several displays and controls which permit complete operation of the antenna. A low cost computer driven CRT display with an associated keyboard and some special control functions can be used to replace the present control console. It is anticipated that such an approach will enhance human engineering aspects of antenna control and will also represent considerable savings when antenna procurements are considered. The CRT display approach is under investigation, but is not reported here.

Details of the program structure and techniques are covered in reference 3.1.

3.1 Digital Compensation

The tracking loop in all modes of operation is closed via the servo amplifier. Inputs are command signals and signals from feedback transducers while the output is a voltage which drives the valve of the hydraulic drive system. In the servo amplifier the drive signal is shaped in accordance with stability and tracking accuracy requirements. This signal shaping is performed by operational amplifiers using input and feedback networks consisting of resistors and capacitors. Inherently, such analog circuitry is subject to drift, noise and

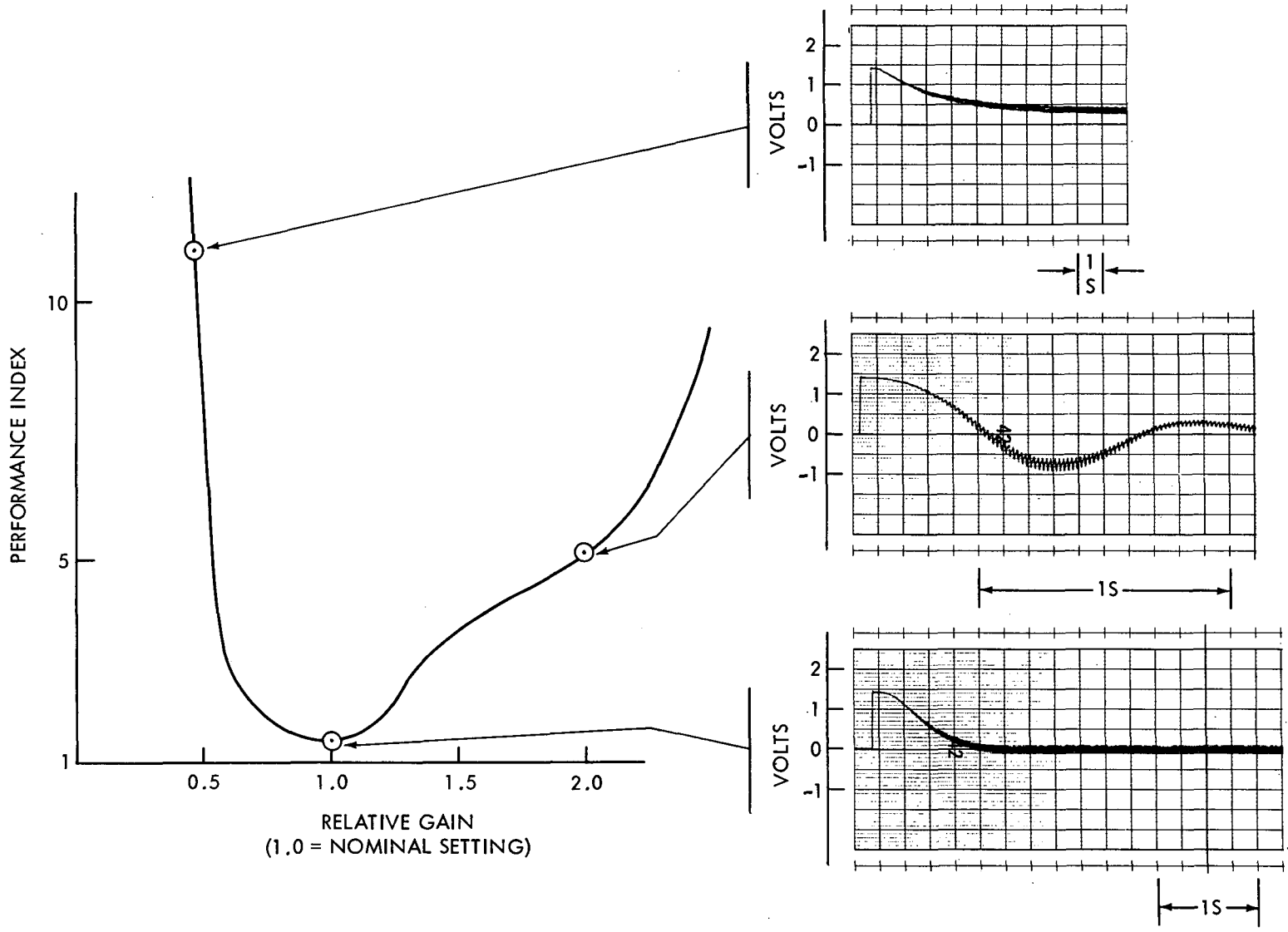

Figure 2-4. Performance Index for Position Loop, Type 1

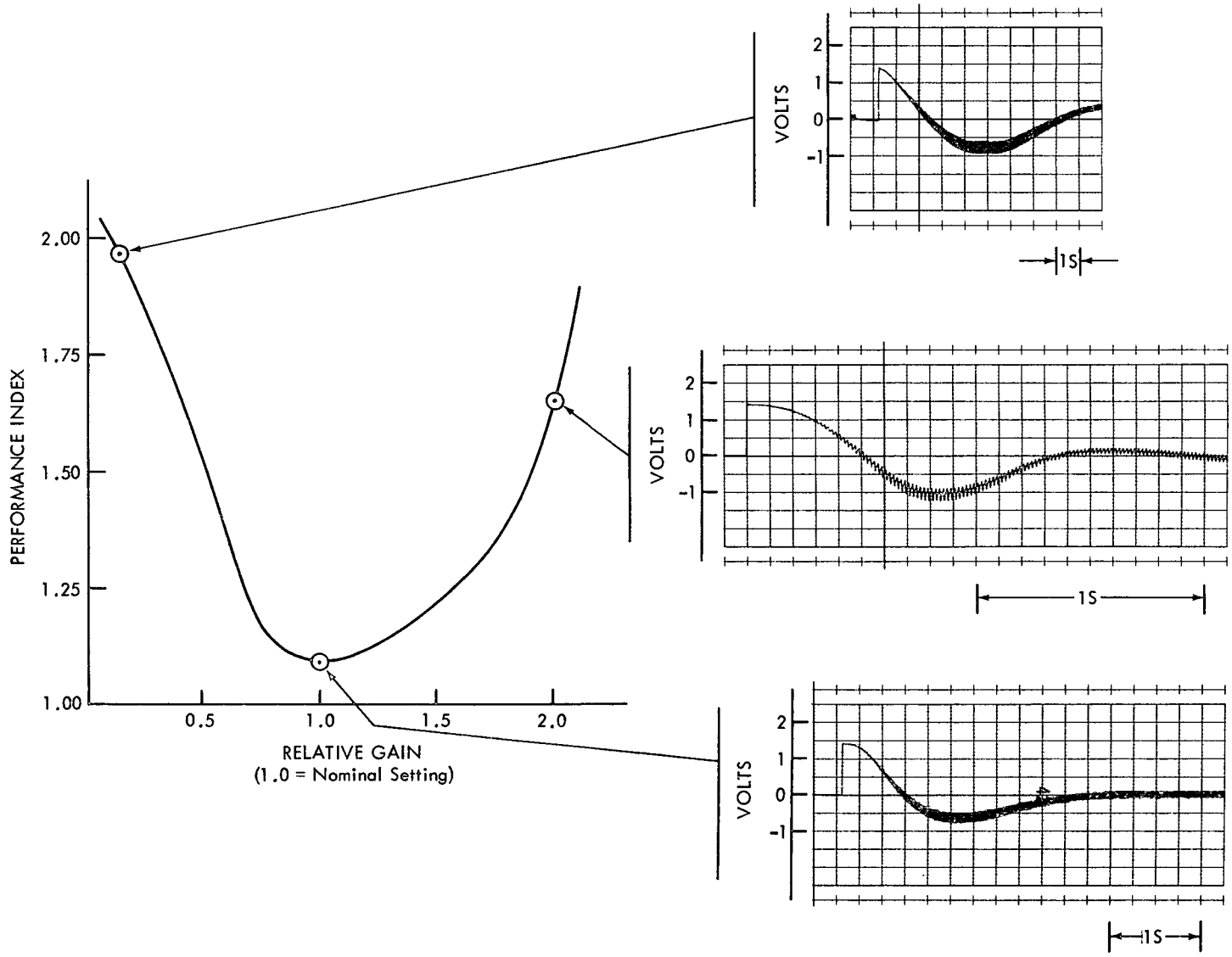

Figure 2-5. Performance Index for Position Loop, Type II

component aging. Replacement of the analog servo amplifier with digital techniques will improve reliability and reduce maintenance requirements.

The block diagram of the analog servo amplifier using Laplace notation is shown in Figure 3.1. In order to implement these characteristics into a digital computer program it is necessary to convert the Laplace expressions into the Z-domain. To ease computational complexity, the block diagram is redrawn in Figure 3.2 with a slightly different arrangement leaving dynamic characteristics unchanged. Next a sampling frequency has to be established which is limited by the computer speed on one extreme and the computational accuracy on the other. The tracking loop has a bandwidth of approximately 1.0 Hz, however substantial attenuation is realized only after the first natural frequency of the structure which is around 5 Hz. Hence a sampling frequency of 20 Hz has been chosen.

Conversion to the Z-domain follows a procedure outlined in reference 3.2 (page 465 and following). This procedure makes use of the W-transform where

$$w = \frac{z - 1}{z + 1} \tag{3.1}$$

$$v = \tan \frac{\omega T}{2} \tag{3.2}$$

where

ω = any frequency in S-domain, rad/sec

v = corresponding frequency in W-domain rad/sec

T = sampling period, sec

The W-transform of A(s) can be found by making use of equation 3.2:

$$A(s) = \frac{1.96}{0.47\ S + 1}$$

$$v = \tan \frac{\left(\frac{1}{0.47}\right)\left(\frac{1}{20}\right)}{2} = 0.0532 \text{ rad/s}$$

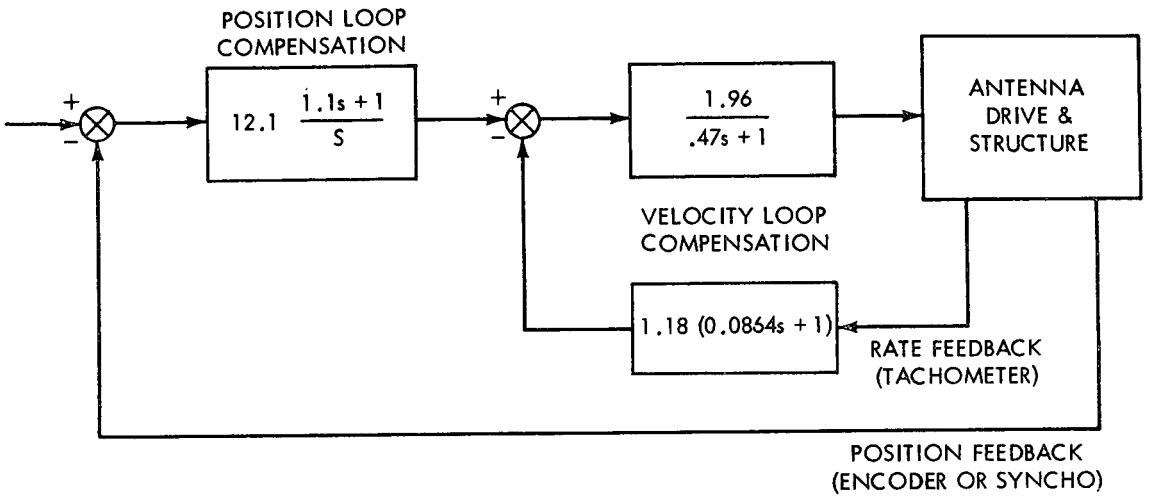

Figure 3-1. Block Diagram of Analog Servo Amplifier

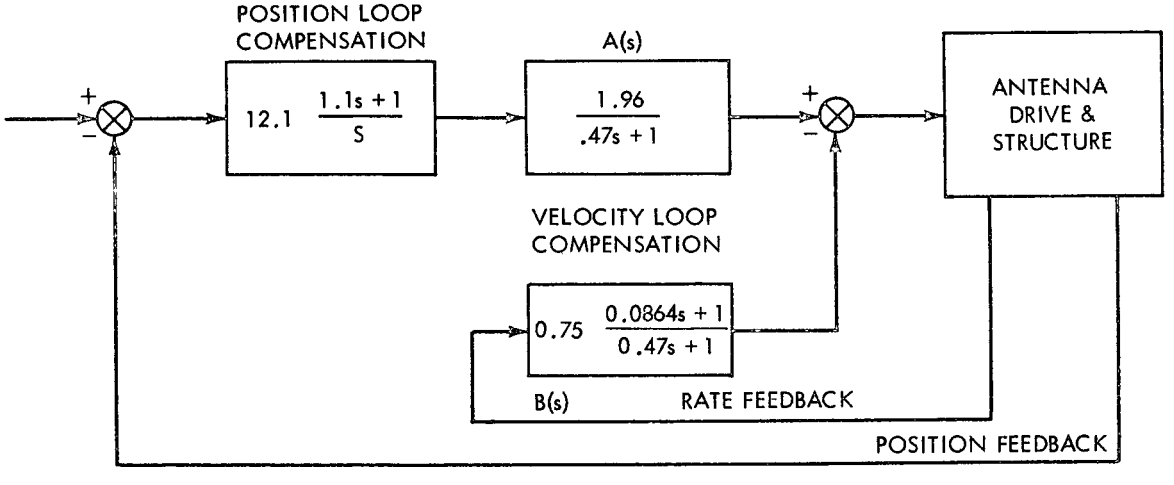

Figure 3-2. Modified Block Diagram of Analog Servo Amplifier

$$A(W) = \frac{1.96}{\frac{W}{0.0532} + 1} = \frac{1.96}{18.9\,W + 1}$$

Substitution of equation (3.1) into above expression yields the desired Z-transform:

$$A(Z) = \frac{1.96}{18.9\,\frac{Z-1}{Z+1} + 1} = \frac{0.099\,Z + 0.099}{Z - 0.899} \tag{3.3}$$

In similar fashion B(s) and C(s) can be converted:

$$B(s) = 0.75\,\frac{0.0864\,s + 1}{0.47\,s + 1}$$

$$B(Z) = \frac{0.165\,Z - 0.089}{Z - 0.899} \tag{3.4}$$

and

$$C(s) = 12.1\,\frac{1.1\,s + 1}{s}$$

$$C(Z) = \frac{13.62\,Z - 13.0}{Z - 1} \tag{3.5}$$

Equations (3.3), (3.4) and (3.5) appear in the general form of:

$$G(Z) = \frac{a_0\,Z + a_1}{Z + b_1}$$

which lends itself readily for computer implementation. If a signal E_{in} (nT) is applied to G(Z), then the output E_{out} (nT) is given by:

$$E_{out}(n\,T) = a_0\,f(n\,T) + a_1\,f[(n-1)\,T]$$

$$f(n\,T) = E_{in}(n\,T) - b_1\,f[(n-1)\,T]$$

where T = sampling period, seconds

n = number of sampling interval

= 0, 1, 2, 3 . . .

Figure 3.3a shows the step function response of the antenna using the analog servo amplifier and digital compensation. Figure 3.3b shows stepfunction responses using digital compensation for various sampling rates. Note that the selection of 20 samples per second is satisfactory.

The digital compensation scheme is based on investigations reported in reference 3.3.

3.2 Antenna Position Program

In conventional tracking stations the Antenna Position Programmer (APP) is used to point the antenna in accordance with satellite predict data. This is accomplished by accepting predicts from the ENV to XY conversion program (covered in paragraph 3.3) interpolating the data and subtracting the antenna encoder reading. The resultant signal is an error which is fed to the servo amplifier. Whenever the antenna operates in this configuration, it is said to be in program mode. The APP is really a special purpose digital machine that accomplishes the tasks outlined.

The function of the APP can be replaced by a program under the computer controlled antenna concept. Figure 3.4 shows the basic block diagram of the position programming function. The program accepts predict data at a one per second rate and synchronizes it with real time. The operator biases real time from the control console. Synchronized data is linearly interpolated to 20 data points per second. The operator can add position bias to this data. Subsequently the data is checked against physical limits of the antenna mount. Then the difference is formed between this quantity and the encoder reading. The resultant error is checked for its maximum limits and fed to the servo amplifier (or digital compensation program).

Mathematically these relationships can be expressed as following: Time Bias:

$$X^1_{pn} = X_{p\,(n+T_{bias})}, \quad n = 0,\ 1,\ 2, \ldots$$

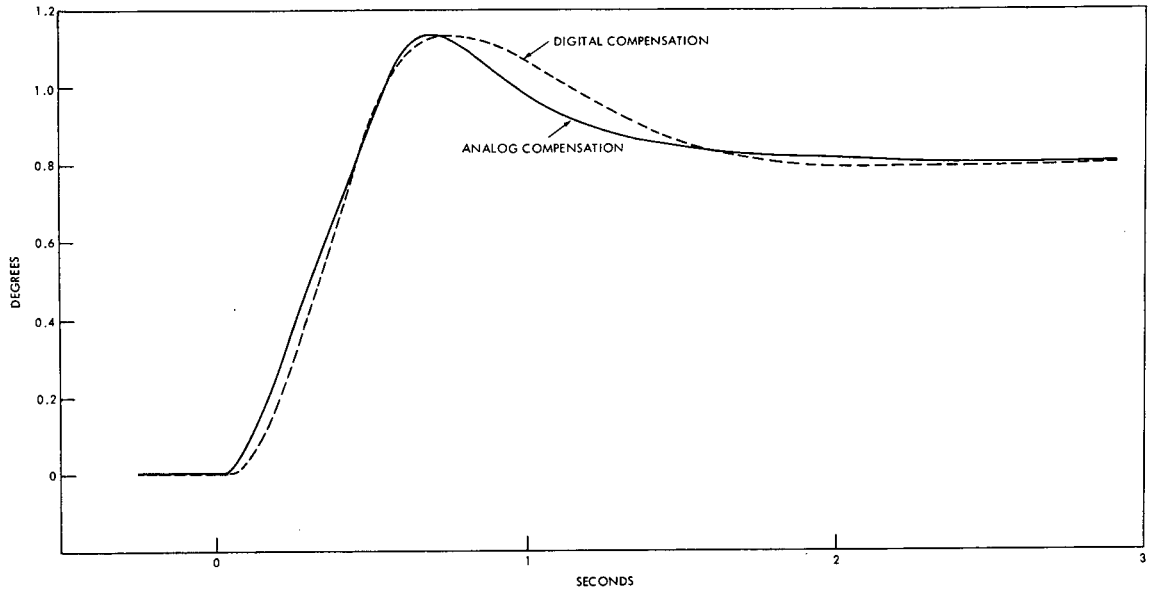

Figure 3-3a. Stepfunction Response of Antenna Using Analog and Digital Compensation (20 samples per second)

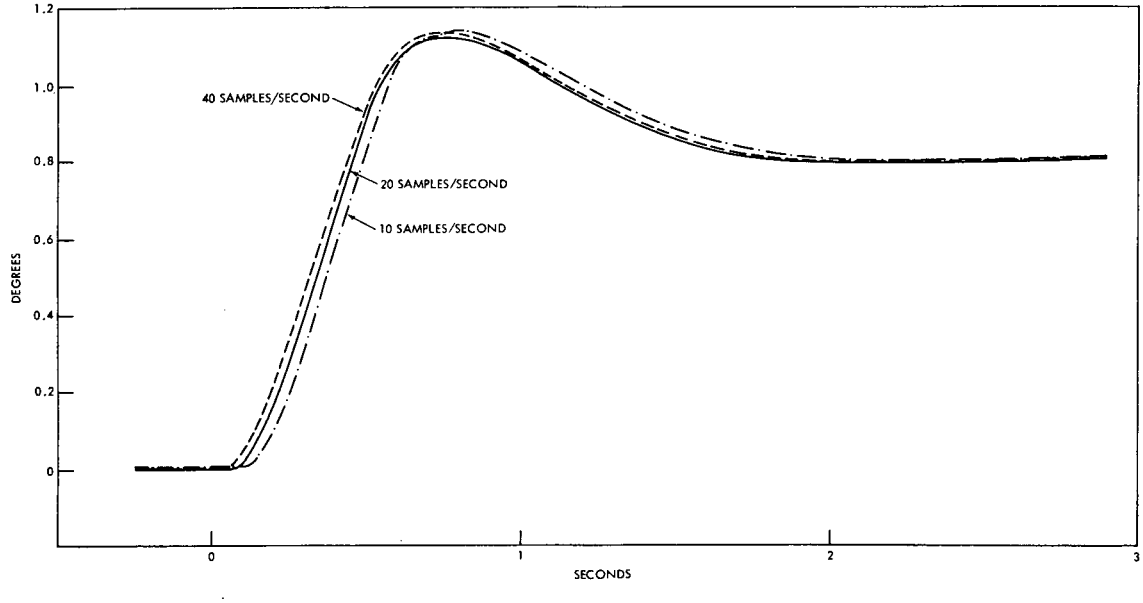

Figure 3-3b. Stepfunction Response of Antenna Using Digital Compensation and Varying Sampling Rate

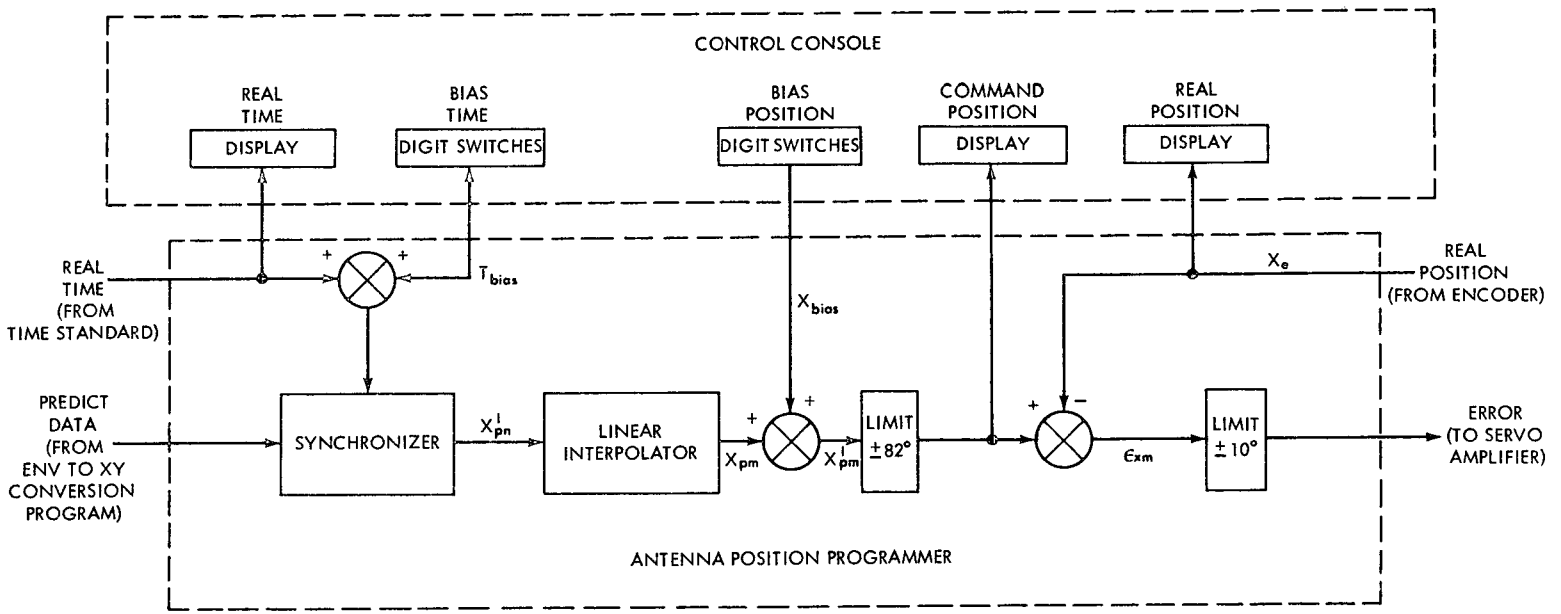

Figure 3-4. Block Diagram of Antenna Position Programming

where

X_{pn} = synchronized predict value at time interval n

X^1_{pn} = synchronized predict value modified by time bias

T_{bias} = time bias introduced by operator

Interpolation:

$$X_{pm} = X^1_{pn} + \left(\frac{X^1_{p(n+1)} - X^1_{pn}}{20} \right) m\,T, \quad m = 0,\ 1,\ \ldots\ 19$$

where

T = sampling interval = 1/20 second

X_{pm} = predict value at time $n + \frac{m}{20}$

Position Bias:

$$X^1_{pm} = X_{pm} + X_{bias}$$

where

X_{bias} = position bias introduced by operator

X^1_{pm} = predict value at time $n + \frac{m}{20}$ modified by position bias

Servo Error:

$$E_{xm} = X^1_{pm} - X_{em} + X_{corr}$$

where

X_{em} = encoder reading at time interval $n + \frac{m}{20}$

X_{corr} = constant for encoder correction

E_{xm} = servo error at time interval $n + \frac{m}{20}$

In addition to the task described above this program drives the console displays as indicated in Figure 3.4. A history record is also generated which permits recording of such quantities: servo error, antenna position and velocity, agc values, and time. The history record can be used for post-pass analysis.

3.3 ENV to XY Conversion

To aid satellite acquisition and tracking, prediction information has to be made available to the antenna system. Orbit calculations for satellites are made on the centralized computer complex at GSFC. Prediction information is transmitted from here to the various tracking stations. However, to save on transmission volume, local processing of prediction data is necessary which involves coordinate conversion and interpolation. This manipulating of data is handled by the PB250 computer at tracking station (UNIVAC 1248 for USB antennas). Under the Computer Controlled Antenna concept this function is handled off-line by the antenna system computer.

The position of a satellite is originally determined using orbital elements in an $E'N'V'$ (East, North, Vertical) coordinate system. The V'-axis is perpendicular to the mean earth equatorial plane and points to the north celestial pole. The E' and N' axes lie in the mean earth equatorial plane. The N' axis points toward the mean vernal equinox and the E' axis is situated to complete a right-hand coordinate system. The origin of this system is at the center of the earth. This system is then rotated and transformed into a topocentric ENV coordinate system with respect to the particular tracking site. In this system the V axis is directed along the upward vertical; the E axis along the eastward horizontal; and the N axis along the northward horizontal.

The ENV vectors for a specific satellite are annotated with time and transmitted to the tracking station. Transmission is limited to a maximum of 75 coordinate values for a particular pass of a particular satellite. This limitation also establishes the spacing of coordinate values in time. This spacing can vary from 1 to 20 minutes depending on the satellite orbit. Figure 3.5 shows a typical record that has been transmitted to a station. Predicts are generated for two weeks in advance and are transmitted to the station.

In the Computer Controlled Antenna concept predicts as shown in Figure 3.5 are accepted and converted to predict records compatible with the antenna position program. The first step in this process is the conversion of ENV data to XY angular data which is accomplished using the following relationships:

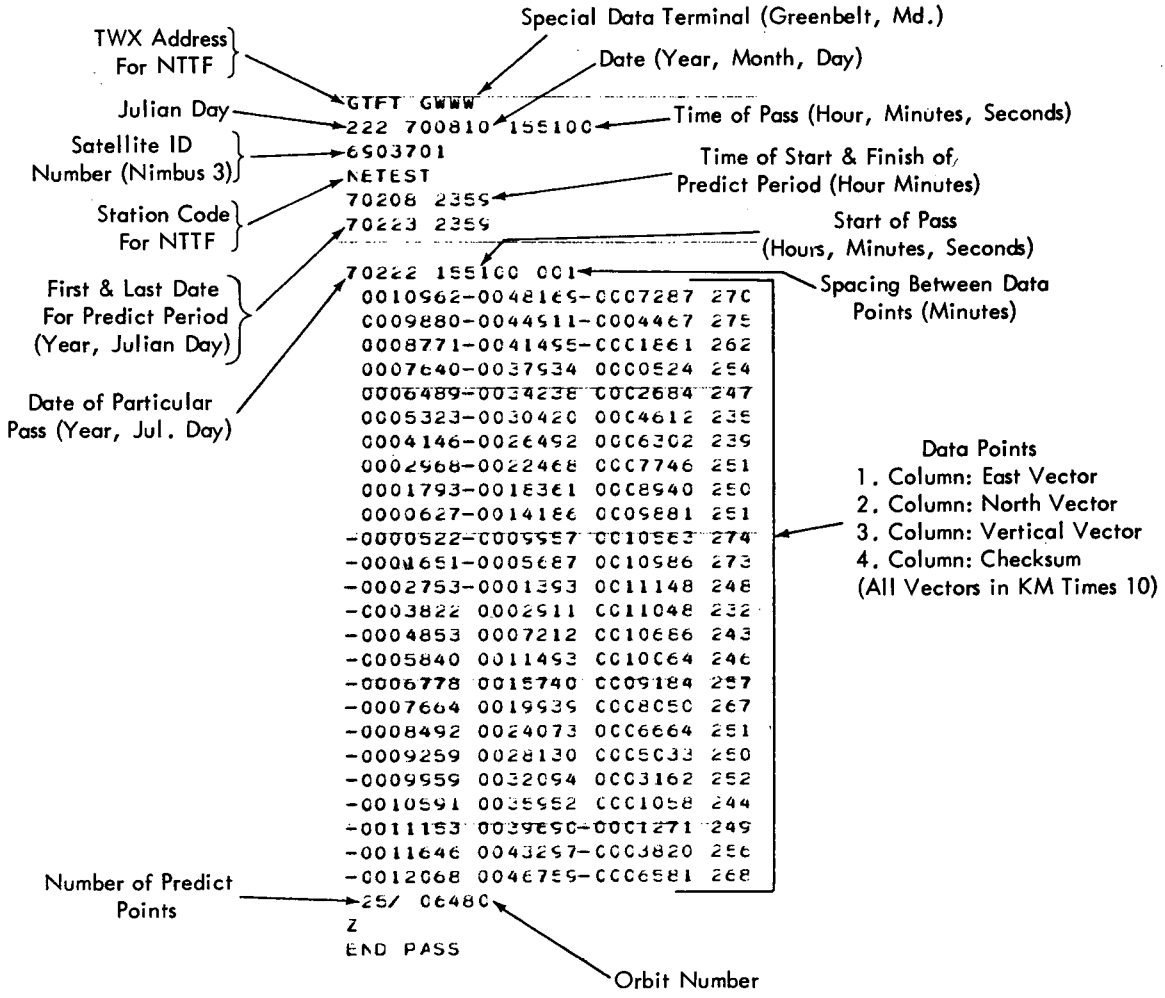

Figure 3-5. Typical Predict Data Format as Sent to a Tracking Station

$$X = \text{arc tan} \frac{E}{V}$$

$$Y = \text{arc tan} \frac{N}{\sqrt{E^2 + V^2}}$$

Some additional conversions are performed which are useful in describing the particular pass to the operator. These are range, R; range rate, $\dot{R}$; azimuth, A; and elevation, E.

$$R = \sqrt{E^2 + N^2 + V^2}$$

$$\dot{R} \approx \frac{R_{present} - R_{previous}}{\text{Time interval}}$$

$$A = \text{arc tan} \frac{E}{N}$$

$$E = \text{arc tan} \frac{V}{\sqrt{E^2 + N^2}}$$

USB antennas are provided with an acquisition message that provide values for x and y angles directly, hence above conversions are not necessary. Using computed or provided X and Y angles with a period, T_Q, between subsequent values, the data is interpolated to yield a fixed predict rate of one per second. The method employed is based on the Lagrange Five Point Interpolation Formula (Reference 3.4; Formula 25.2.15) which is given by:

$$X_t = \frac{1}{24}(t^2 - 1)\, t\, (t - 2)\, a_0 - \frac{1}{6}(t - 1)\, t\, (t^2 - 4)\, a_1$$

$$+ \frac{1}{4}(t^2 - 1)(t^2 - 4)\, a_2 - \frac{1}{6}(t + 1)\, t\, (t^2 - 4)\, a_3$$

$$+ \frac{1}{24}(t^2 - 1)\, t\, (t + 2)\, a_4 \qquad (3.6)$$

where

a_0, a_1, a_2, a_3, a_4 = interpolation coefficients

t = normalized time

x_t = angular value at time t

Interpolation about a specific predict point, $X_{q=0}$, is accomplished by evaluating the interpolation coefficients first using $X_{q=0}$ and two points on either side of $X_{q=0}$. Evaluation of equation (3.6) at t = -2, -1, 0, 1, 2 and equating appropriate terms to predict values

$$X_{t=-2} = a_0 = X_{q=-2}$$

$$X_{t=-1} = a_1 = X_{q=-1}$$

$$X_{t=0} = a_2 = X_{q=0}$$

$$X_{t=1} = a_3 = X_{q=1}$$

$$X_{t=2} = a_4 = X_{q=2} \tag{3.7}$$

Rearranging equation (3.6) gives:

$$x_t = b_0 + b_1 t + b_2 t^2 + b_3 t^3 + b_4 t^4 \tag{3.8}$$

where

$$b_0 = a_2$$

$$b_1 = \frac{1}{12} a_0 - \frac{2}{3} a_1 + \frac{2}{3} a_3 - \frac{1}{12} a_4$$

$$b_2 = -\frac{1}{24} a_0 + \frac{2}{3} a_1 - \frac{5}{4} a_2 + \frac{2}{3} a_3 - \frac{1}{24} a_4$$

$$b_3 = -\frac{1}{12} a_0 + \frac{1}{6} a_1 - \frac{1}{6} a_3 + \frac{1}{12} a_4$$

$$b_4 = \frac{1}{24} a_0 - \frac{1}{6} a_1 + \frac{1}{4} a_2 - \frac{1}{6} a_3 + \frac{1}{24} a_4$$

Coefficients b_0 through b_4 can be numerically evaluated using relationships in (3.7). Predict angles at a one per second rate can now be generated by subsequent solutions of equation (3.8) for different values of time, t, such that:

$$t = \frac{n}{60\,T_q} - \frac{1}{2}; \quad n = 0,\ 1,\ 2 \ldots (60\,T_q - 1)$$

where T_q = spacing between predict values in whole minutes ($1 \leq T_q \leq 20$).

After computation of $60\,T_q$ predict values new interpolation coefficients are established, by dropping the last predict value, $X_{q=-2}$, and using new point $X_{q=3}$. This process is then continued until the whole pass has been covered.

3.4 Scan Pattern

To aid in the acquisition phase antennas are provided with a scan generator. This generator superimposes a search pattern in most modes of operation. The pattern used most frequently is that of an Archimedes spiral. Conventionally, implementation of this pattern is accomplished by using electromechanical devices such as a sine-cosine pot or a resolver and an electrical or mechanical integrator. In the computer controlled antenna the equation for a spiral is solved and then added to the current X and Y angles of the antenna. The equation for a spiral is given by:

$$X = a\,t \cos \omega t$$

$$Y = a\,t \sin \omega t \qquad (3.9)$$

where

a = spiral width

ω = spiral angular frequency.

The difficulty with this equation is that the tangential velocity changes. This change is undesirable when one investigates acquisition probabilities but is difficult to overcome with the electromechanical scan generator. In the computer controlled antenna concept this shortcoming can be eliminated. The tangential velocity, v , can be kept essentially constant by making a substitution into equation (3.9):

$$X = a\, z \cos \omega z$$

$$Y = a\, z \sin \omega z \qquad (3.10)$$

where

$$Z = f(t)$$

The tangential velocity is given by:

$$v = \sqrt{\dot{x}^2 + \dot{y}^2} \qquad (3.11)$$

The derivatives of equation (3.10) are:

$$\dot{X} = a\, \dot{z} \cos \omega z - a\, \omega z\, \dot{z} \sin \omega z$$

$$\dot{Y} = a\, \dot{z} \sin \omega z + a\, \omega z\, \dot{z} \cos \omega z$$

substitution of these derivatives into (3.11) yields:

$$v = a\, \dot{z} \sqrt{1 + \omega^2 z^2}$$

and

$$v \approx a\, \omega z\, \dot{z}$$

for values of z such that

$$\omega^2 z^2 >> 1.$$

A function that satisfies v = constant is

$$z = \sqrt{t} \quad \text{and} \quad \dot{z} = \frac{1}{2} \frac{1}{\sqrt{t}}$$

If the spiral is adjusted to 2-1/2 turns then

$$\omega z_{max} = 5\pi$$

and defining a maximum radius, r_{max} :

$$r_{max} = az_{max}$$

it is possible to find expressions for constants a and ω in equation (3.10):

$$a = 0.36\sqrt{v\, r_{max}}$$

$$\omega = 5.6\sqrt{\frac{v}{r_{max}}}$$

Hence the scan pattern implemented on the computer is:

$$X = 0.36\sqrt{v\, r_{max}}\; t \cos\left[5.6\sqrt{\frac{v\, t}{r_{max}}}\right]$$

$$Y = 0.36\sqrt{v\, r_{max}}\; t \sin\left[5.6\sqrt{\frac{v\, t}{r_{max}}}\right]$$

The operator specifies, r_{max}, by setting the scan radius switch on the operators console, while the tangential velocity, v, is fixed at one degree per second. It will be substantially simple to extend this algorithm to one that maximizes acquisition probability by automatically selecting v and r_{max} based on radio-frequency receiver selection. Figure 3.6 shows the scan pattern generated by the above method.

4. AUGMENTATION

The augmentation mode is a combination between autotrack and program mode and displays a tracking error that is less than either of the two other modes. In the augmentation mode use is made of the inherent characteristics of the autotrack and program modes:

Autotrack: Major tracking error due to receiver noise

Program: Major tracking error due to timing inaccuracies and misalignments of antenna radio frequency axis.

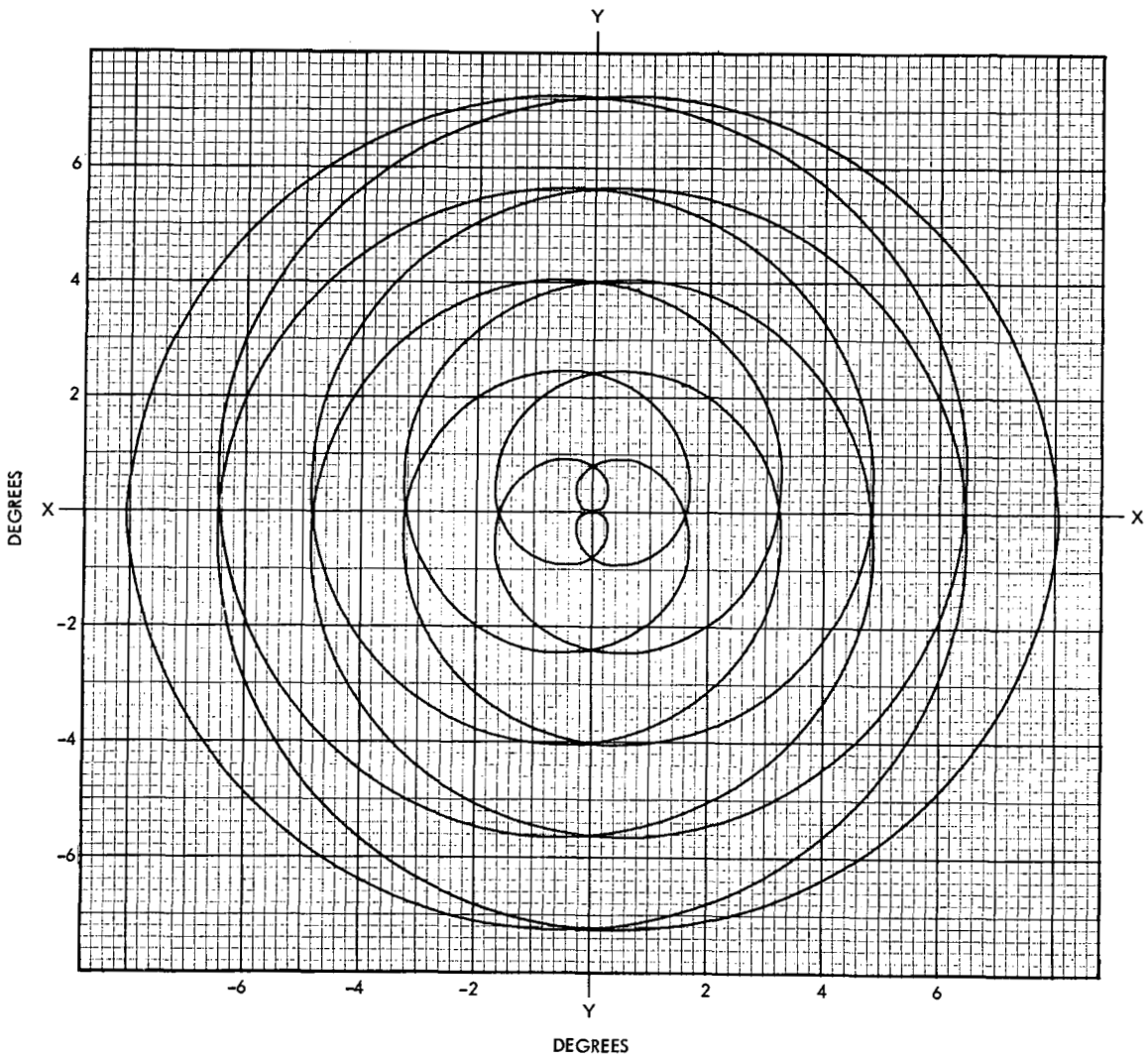

Figure 3-6. Scan Pattern

In order to analyze this mode of operation a satellite in a 160.9 km (100 mile) circular orbit is assumed passing directly over the tracking antenna. Tracking errors in the various modes of operation will be evaluated and compared with each other.

4.1 Satellite Motion

In order to analyze the tracking performance of the antenna equivalent sinusoidal inputs will be used. These inputs are computed using a technique described in reference 4.1 (page 43 and following). Use of sinusoidal inputs simplifies computational manipulations. The orbital velocity of the satellite is established using:

$$v = \sqrt{\frac{k}{r}}$$

where

v = velocity of satellite, km/s

k = gravitational constant

= 398,297.83 km^3/s^2

r = semimajor axis

= earth radius + satellite height

= 6377.8 + 160.9 = 6538.7 km

Hence

$$v = \sqrt{\frac{398.297}{6538.7}} = 7.805 \text{ km/s}$$

A normalization constant, a, can be computed

$$a = \frac{v}{h} = \frac{7.805}{160.9} = 0.0485 \text{ 1/s}$$

where

h = satellite height = 160.9 km

The equivalent sinusoid for antenna position is given by:

$$\theta_{sp}(t) = A_p \sin \omega_{sp} t$$

where

$\theta_{sp}(t)$ = amplitude of equivalent sinusoid due to position changes, rad

A_p = peak amplitude of equivalent sinusoid due to position changes, rad

ω_{sp} = frequency of equivalent sinusoid due to position changes, rad/s

From a curve given in reference 4.1 (page 46)

$$A_p = 0.64 \times 2 = 1.28 \text{ rad}$$

$$\omega_{sp} = \frac{2\pi}{12} a = \frac{2\pi}{12} \times 0.0485 = 0.0254 \text{ rad/s}$$

Similarly, using subscripts v, a, and j for velocity, acceleration, and jerk respectively

$$A_v = 0.5\, a = 0.0243 \text{ rad/s}$$

$$\omega_{sv} = \frac{2\pi}{3.6} a = 0.0846 \text{ rad/s}$$

$$A_a = 0.65\, a^2 = 0.00153 \text{ rad/s}^2$$

$$\omega_{sa} = \frac{2\pi a}{2.0} = 0.152 \text{ rad/s}$$

$$A_j = 0.6\, a^3 = 0.0000685 \text{ rad/s}^3$$

$$\omega_{sj} = \frac{2\pi a}{1.0} = 0.305 \text{ rad/s}$$

Hence the equivalent sinusoids for the stipulated satellite are:

$$\theta_{sp}(t) = 1.28 \sin 0.0254\, t$$

$$\theta_{sv}(t) = 0.0243 \sin 0.0846\, t$$

$$\theta_{sa}(t) = 0.00153 \sin 0.152\, t$$

$$\theta_{sj}(t) = 0.0000685 \sin 0.305\, t$$

4.2 Servo Loop

Before discussing a particular mode of operation it is necessary to analyze the servo loop without considering receiver, prediction and alignment errors. As was shown in paragraph 3.1 the basic servo loop is a type II servo. Such a servo can be stabilized by a simple lead-lag network and has an open loop transfer function G_{so}:

$$G_{so} = \frac{K\, a\, (T_1\, s + 1)}{s^2\, (T_2\, s + 1)}$$

where

K_a = acceleration gain, 1/seconds^2

T_1 = time constant of lead, seconds

T_2 = time constant of lag, seconds

For a phase margin of 0.662 rad and a damping factor of 0.5 the following relationships can be established with the crossover frequency, ω_c:

$$K_a = \frac{1}{2}\omega_c^2$$

$$\frac{1}{T_1} = \frac{\omega_c}{2} \qquad \frac{1}{T_2} = 2\,\omega_c$$

Hence the open loop transfer function can be rewritten:

$$G_{so} = \frac{\frac{1}{2}\omega_c^2 \left(\frac{2}{\omega_c} s + 1\right)}{s^2 \left(\frac{1}{2\omega_c} s + 1\right)} \tag{4.1}$$

The closed loop transfer function, G_s, can be found:

$$G_s = \frac{G_{so}}{1 + G_{so}} = \frac{\frac{2}{\omega_c} s + 1}{\left(\frac{1}{\omega_c} s + 1\right)\left(\frac{1}{\omega_c^2} s^2 + \frac{1}{\omega_c} s + 1\right)} \tag{4.2}$$

Similarly the error transfer function can be established:

$$\frac{\epsilon_s(s)}{\theta_c(s)} = \frac{1}{1 + G_{so}} = \frac{2 \; s^2 \left(\frac{1}{2\omega_c} s + 1\right)}{\omega_c^2 \left(\frac{1}{\omega_c} s + 1\right)\left(\frac{1}{\omega_c^2} s^2 + \frac{1}{\omega_c} s + 1\right)} \tag{4.3}$$

where

ϵ_s = servo error, rad

θ_c = command angle input, rad

Assuming sinusoidal excitation:

$$\theta_c(t) = A \sin \omega_s t$$

$$\theta_c(s) = \frac{A}{\omega_s} \frac{1}{1 + \frac{1}{\omega_s^2} s^2}$$

the error in equation (4.3) can be expressed as:

$$\epsilon_s(s) = \frac{2}{\omega_c^2}\,\frac{A}{\omega_s}\left[\frac{S^2\left(\frac{1}{2\,\omega_c}\,s+1\right)}{\left(\frac{1}{\omega_c^2}S^2+\frac{1}{\omega_c}S+1\right)\left(\frac{1}{\omega_c}S+1\right)\left(\frac{1}{\omega_s^2}s^2+1\right)}\right]$$

Using partial fraction expansion $\epsilon(s)$ can be written as:

$$\epsilon_s(s) = \omega_s A\left[\frac{k_1}{S+\frac{\omega_c}{2}+j\frac{\omega_c}{2}\sqrt{3}} + \frac{k_1^*}{s+\frac{\omega_c}{2}-j\frac{\omega_c}{2}\sqrt{3}}\right.$$

$$\left. + \frac{k_2}{s+\omega_c} + \frac{k_3}{s+j\,\omega_s} + \frac{k_3^*}{s-j\,\omega_s}\right]$$

where the * indicates the complex conjugate.

By inspection, only k_3 terms will yield a steady state response, hence

$$\epsilon_s(s)\Big|_{\text{steady state}} = \left[\frac{k_3}{s+j\,\omega_s} + \frac{k_3}{s-j\,\omega_s}\right]\omega_s A \tag{4.4}$$

and

$$k_3 = \left.\frac{s^2(s+2\,\omega_c)}{(s^2+\omega_c\,s+\omega_c^2)(s+\omega_c)(s+j\,\omega_s)}\right|_{s=j\,\omega_s}$$

$$= -\frac{\omega_s}{2}\,\frac{(\psi\,\omega_c^2+\omega_s^2)^{1/2}\,\epsilon^{j\psi_1}}{[\omega_s^2(\omega_s^2-2\,\omega_c^2)^2+\omega_c^2(\omega_c^2-2\,\omega_s^2)]^{1/2}\,\epsilon^{j\,\psi_2}}$$

where

$$\tan \psi_1 = \frac{\omega_s}{2\,\omega_c} \quad ; \quad \tan \psi_2 = \frac{\omega_c\,(\omega_c^2 - 2\,\omega_s^2)}{\omega_s\,(\omega_s^2 - 2\,\omega_c^2)}$$

$$\psi = \psi_1 - \psi_2$$

Transformation of equation (4.4) into the time domain yields:

$$\epsilon_s(t)\Big|_{\text{steady state}} = -\,\omega_s^2\,A\left[\frac{(4\,\omega_c^2 + \omega_s^2)^{1/2}}{[\omega_s^2\,(\omega_s^2 - 2\,\omega_c^2)^2 + \omega_c^2\,(\omega_c^2 - 2\,\omega_s^2)^2]^{1/2}}\right]\cos(\omega_s\,t + \psi)$$

and for the case $\omega_s << \omega_c$:

$$\epsilon_s(t)\Big|_{\text{steady state}} = -\,2\frac{\omega_s^2}{\omega_c^2}\,A\cos(\omega_s\,t + \psi) \tag{4.5}$$

Amplitude A and frequency ω_s of the excitation have been established in paragraph 4.1. There remains the crossover frequency, ω_c, to be found. This can be done following the procedure in reference 4.1. An approximate transfer function established by satellite motion can be found using the results from paragraph 4.1 and is shown graphically in Figure 4.1. Adjusting the gain of transfer function G_{so} such that the approximate transfer function is below G_{so} and $\omega_c = 6.28$ rad/s is found. This indeed represents the design value of most STDN antennas. It should also be noted that the design as chosen provides sufficient attenuation for the structural natural frequency of the antenna which occurs around 5.0 Hz.

The maximum steady state errors can now be computed using equation (4.5)

$$\epsilon_s/\text{position} = 2\,\frac{0.0254^2}{6.28^2}\,(1.28) = 0.0419 \text{ m rad}$$

$$\epsilon_s/\text{velocity} = 2\,\frac{0.0846^2}{6.28^2}\,(0.0243) = 0.00879 \text{ m rad}$$

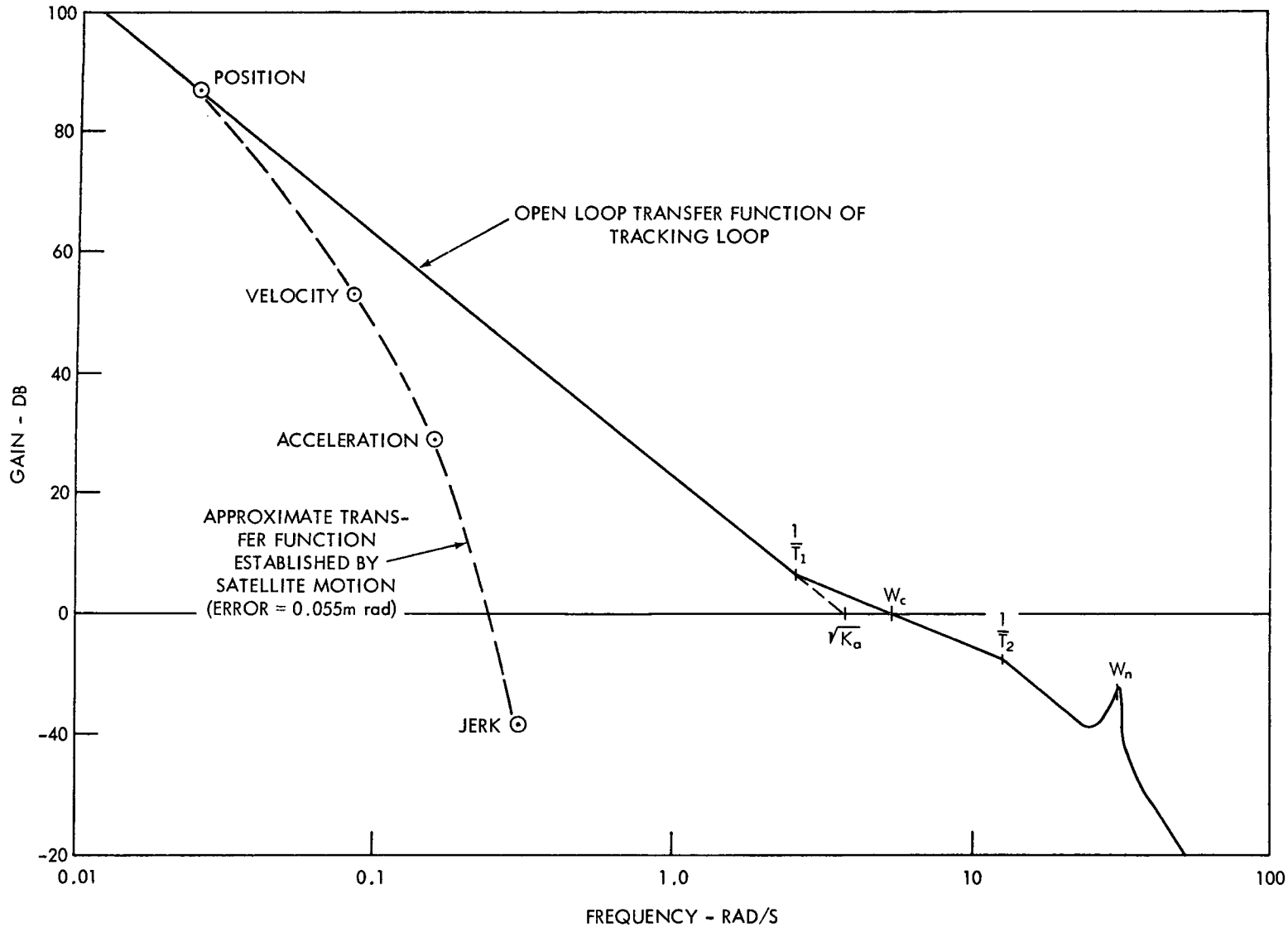

Figure 4-1. Bode Plot for Tracking Loop

$$\epsilon_s/\text{acceleration} = 2\,\frac{0.152^2}{6.28^2}\,(0.00152) = 0.00178 \text{ m rad}$$

$$\epsilon_s/\text{jerk} = 2\,\frac{0.305^2}{6.28^2}\,(0.0000685) = 0.000323 \text{ m rad}$$

As can be seen from above the major servo error is due to the equivalent sinusoid of position.

4.3 Autotrack Mode

Next the operation of the antenna in the autotrack mode will be considered. Operation in this mode is essentially identical to that of the closed loop servo analyzed in the previous paragraph. The only difference is a receiver noise term that has to be added to the loop. But before discussing the autotrack loop, the pertinent receiver characteristic will be established. The assumption is made that the noise power spectrum, ϕ_{rr}, is flat up to a frequency, ω_r, which is the bandwidth of the receiver error channel and that the spectrum has an amplitude K_R. Hence the spectrum can be expressed mathematically:

$$\phi_{RR} = K_R\,\frac{\omega_R^2}{\omega_R^2 + \omega^2} \tag{4.6}$$

If the additional assumption is made that the root-mean-square noise of the receiver, E_{RR} (rms), has a value of 2 mrad and that the error channel bandwidth is 62.8 rad/s (ten times servo bandwidth) then K_R can be evaluated:

$$\epsilon_{RR}\,(\text{rms})^2 = \int_0^\infty \phi_{RR}\,(\omega)\,d\,\omega = \frac{\pi\,k_R\,\omega_R}{2}$$

and

$$K_R = \frac{2\,\epsilon_{RR}\,(\text{rms})^2}{\pi\,\omega_R} = \frac{2 \times 4}{62.8\,\pi} = 0.00404 \text{ m rad}^3/\text{S}$$

The tracking error in the autotrack mode can be found by applying the superposition theorem. The tracking error is the sum of the error due to satellite motion alone and the error due to receiver noise alone. The first error is the servo error, E_s, established in the previous paragraphs while the second error component, E_R, will be developed below. Using reference 4.2 as a basis:

$$\epsilon_R^2 = \frac{1}{2\pi j} \int_{-j\infty}^{j\infty} |G_s(s)|^2 \phi_{RR}(s)\, ds$$

$G_s(s)$ is the closed loop transfer function developed previously and is given in equation (4.2). The spectrum $\phi_{RR}(s)$ is the transform of spectrum $\phi_{RR}(\omega)$ given by (4.6). Hence above expression can be rewritten as:

$$\epsilon_R^2 = k_R\, \omega_c^4\, \omega_4^2\, \frac{1}{2\pi j} \int_{-j\infty}^{j\infty} \left| \frac{2 s \omega_c}{s^3 + 2\omega_c s^2 + \omega_c^3} \right|^2 \frac{ds}{s^2 + \omega_R^2}$$

This expression can be put into a form compatible with reference (4.2) (Appendix E):

$$\epsilon_R^2 = k_R\, \omega_c^4\, \omega_R^2\, \frac{1}{2\pi j} \int_{-j\infty}^{j\infty} \frac{C(s)\, C(-s)}{d(s)\, d(-s)}\, ds \qquad (4.7)$$

$$= k_R\, \omega_c^4\, \omega_R^2\, I_R$$

where

$$c(s) = 2s + \omega_c$$

$$d(s) = s^4 + (2\omega_c + \omega_R)\, s^3 + 2\omega_c (\omega_c + \omega_R)\, s^2 + \omega_c^2 (\omega_c + 2\omega_R)\, s + \omega_c^3 \omega_R$$

Making use of a previous assumption that $\omega_R = 10\,\omega_c$ the coefficients of the above expression are:

$$c_0 = \omega_c \qquad d_0 = 10\,\omega_c^4$$

$$c_1 = 2 \qquad d_1 = 21\,\omega_c^3$$

$$d_2 = 22\,\omega_c^2$$

$$d_3 = 12\,\omega_c$$

$$d_4 = 1$$

From reference (4.2):

$$I_4 = \frac{C_1^2\, d_0\, d_3\, d_4 + C_0^2\,(-\,d_1\, d_4^2 + d_2\, d_3\, d_4)}{2\, d_0\, d_4\,(-\,d_0\, d_3^2 - d_1^2\, d_4 + d_1\, d_2\, d_3)}$$

Substitution of the coefficients and simplification yields

$$I_4 = 0.00988\,\omega_c^{-5}$$

and substitution of this quantity into (4.7) gives

$$\epsilon_R^2 = 0.988\, K_R\, \omega_c$$

and

$$\epsilon_R = 0.995\sqrt{k_R\,\omega_c} = 0.995\sqrt{(0.00404)\,(6.28)}$$

$$= 0.158 \text{ mrad}$$

4.4 Program Mode

The major errors in the program mode of operation are due to prediction errors and misalignments fo the radio frequency axis of the antenna. Both of these errors are of the dc bias type and therefore are not affected by the operation of the servo. To express this phenomenon mathematically, it is only necessary to consider an input to the servo loop that is the sinusoid due to satellite motion, but shifted by a bias term which is proportional to the error.

The transfer function of the programmer which includes antenna misalignments can be computed by noting that the input is

$$\theta_s (t) = A \sin \omega_s t$$

and the output is

$$\theta_p (t) = A \sin (\omega_s t + \phi)$$

where

ϕ = phase shift proportional to error term.

Since ϕ is generally small, $\sin \phi \approx \phi$ and $\cos \phi \approx 1$. With this θ_p (t) can be expressed:

$$\theta_p (t) = A (\sin \omega_s t + \phi \cos \omega_s t)$$

Taking Laplace transforms:

$$\theta_s (s) = \frac{A}{\omega_s} \frac{1}{1 + \frac{1}{\omega} s^2}$$

$$\theta_p (s) = \frac{1}{\omega_s} \left[\frac{\frac{\phi}{\omega_s} s + 1}{1 + \frac{1}{\omega} s^2} \right]$$

Hence the transfer function, G_p (s), can be found:

$$G_p (s) = \frac{\theta_p (s)}{\theta_s (s)} = \frac{\phi}{\omega_s} s + 1 \qquad (4.8)$$

If the assumption is made that program error, ϵ_p, is equal to autotrack error, then

$$\epsilon_p (t) = \theta_s (t) - \theta_t (t) = - \phi A \cos \omega_s t$$

$$\epsilon_p (t)\Big|_{max} = 0.158 \text{ mrad}$$

The phase shift, ϕ, can be numerically evaluated for the equivalent sinusoid of position:

$$\phi = \frac{0.158}{1.28} \times 10^{-3} = 0.000158 \text{ rad}$$

4.5 Augmentation Mode

The basic approach to this mode of operation is based on an idea and preliminary investigation by G. C. Winston (reference 1.1). In this mode the antenna is operated as if it were in the program mode, but the predicted angle is modified by a term derived from the receiver. This correction term is obtained by passing the receiver error through a low pass filter and then performing an integration. Figure 4.2 shows the basic block diagram of this mode. The augmentation filter has a transfer function:

$$G_f(s) = \frac{k_f}{s(T_f s + 1)}$$

where

k_f = gain of filter

T_f = time constant of filter, s.

The constants will be adjusted such that

$$10 K_f = \omega_c \quad \text{and} \quad T_f = \frac{1}{K_f}$$

Hence,

$$G_f(s) = \frac{\frac{\omega_c}{10}}{s\left(\frac{10}{\omega_c} s + 1\right)} = \frac{K_f^2}{s(s + K_f)} \tag{4.9}$$

Analysis of this mode will make use again of the superposition theorem, i.e., first errors will be computed with receiver noise input only ($\theta_s(t) = 0$) and then with satellite motion only ($\phi_{RR}(\omega) = 0$). The effective transfer function, G_R, to which receiver noise is applied is:

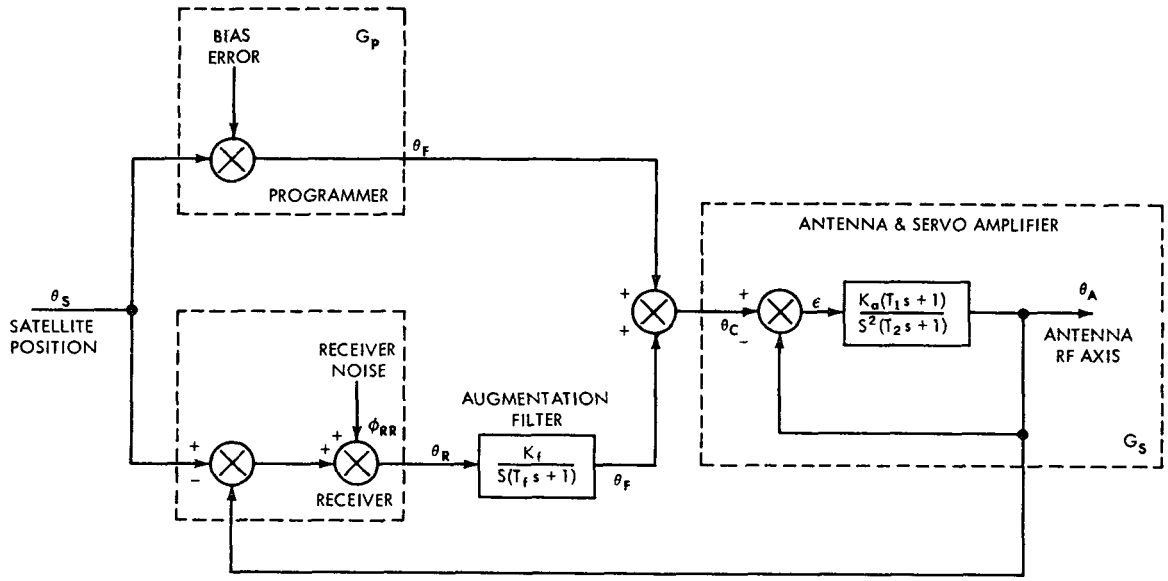

Figure 4-2. Block Diagram for Augmentation Mode

$$G_R(s) = \frac{G_f(s)\, G_s(s)}{1 + G_f(s)\, G_s(s)}$$

From the development of expression (4.8) it can be seen that the bandwidth of the augmentation filter is approximately one tenth of the servo loop. Hence $G_R(s)$ can be simplified and expression (4.9) can be substituted:

$$G_R(s) \approx \frac{G_f(s)}{1 + G_f(s)} = \frac{K_f^2}{s^2 + K_f\, s + K_f^2}$$

Using, again, techniques from reference (4.2) the error due to receiver noise, ϵ_R^1, will be computed:

$$\epsilon_R^{1\,2} = \frac{1}{2\pi j} \int_{-j\infty}^{j\infty} |G_A(s)|^2 \phi_{RR}(s)\, ds$$

$$= K_R K_f^4 \omega_R^2 \frac{1}{2\pi j} \int_{-j\infty}^{j\infty} \left| \frac{1}{s^2 + K_f s + K_f^2} \right|^2 \frac{ds}{s^2 + \omega_R^2}$$

Evaluating the integral and noting:

$$\omega_R = 10\,\omega_C = 100\,k_f$$

the following expression is obtained:

$$(\epsilon_R')^2 = \frac{k_R k_f}{2}$$

and

$$\epsilon_R^1 = 0.707\sqrt{K_R K_f}$$

Using numerical values for K_R and k_f:

$$\epsilon_R^1 = 0.707\sqrt{(0.00404)(0.628)} = 0.0356 \text{ mrad}$$

Next the error due to satellite motion will be investigated. Following the block diagram it can be shown that the transfer function θ_A/θ_s is:

$$\frac{\theta_A(s)}{\theta_s(s)} = \frac{G_s(s)\,G_p(s)}{1 + G_s(s)\,G_F(s)} + \frac{G_s(s)\,G_F(s)}{1 + G_s(s)\,G_F(s)}$$

Using the previous assumption this transfer function can be approximated as

$$\frac{\theta_A(s)}{\theta_s(s)} = \frac{G_p(s)}{1 + G_F(s)} + \frac{G_F(s)}{1 + G_F(s)} + \frac{G_p(s) + G_F(s)}{1 + G_F(s)}$$

The error, ϵ_p^1, under these conditions is:

$$\epsilon_p^1 (s) = \theta_s (s) - \theta_A (s)$$

$$= \frac{1 - G_p (s)}{1 - G_F (s)} \theta_s (s)$$

and substitution of equations (4.8) and (4.9) yields:

$$\epsilon_p^1(s) = \frac{\frac{\phi}{\omega_s} s^2 (s + K_f)}{s^2 + s K_f + K_f^2} \theta_s (s)$$

Applying sinusoidal excitation and using partial fraction expansion:

$$\epsilon_p^1 (s) = \frac{\frac{\phi}{\omega_s} s^2 (s + K_f)}{s^2 + s K_f + K_f^2} \frac{A \omega_s}{s^2 + \omega_s^2}$$

$$= \frac{K_1}{s + \frac{K_f}{2} + j \frac{\sqrt{3}}{2} K_f} + \frac{K_1^*}{s + \frac{K_c}{2} - j \frac{\sqrt{3}}{2} K_f}$$

$$\frac{K_2}{s + j \omega_s} + \frac{k_2^*}{s - j \omega_s}$$

By inspection only K_2 terms will yield a steady state response hence:

$$\epsilon_p^1 (s)\Big|_{\text{steady state}} = \frac{K_2}{s + j \omega_s} + \frac{K_2^*}{s - j \omega_s}$$

where

$$K_2 = \frac{\phi A s^2 (s + K_f)}{(s^2 + s K_f + K_f^2)(s + j \omega_s)} \Bigg|_{s=j\omega_s}$$

$$= \frac{\phi A \omega_s}{2} \left[\frac{(K_f^2 + \omega_s^2)^{1/2} \epsilon^{j\psi_1}}{[\omega_s^2 K_f^2 + (\omega_s^2 - K_f^2)]^{1/2} \epsilon^{j\psi_2}} \right]$$

and where

$$\tan \psi_1 = \frac{\omega_s}{K_f}; \quad \tan \psi_2 = \frac{\omega_s^2 - K_f^2}{\omega_s K_f}; \quad \psi = \psi_1 - \psi_2$$

Conversion into the time domain yields

$$E_p^1 (t)\Big|_{\text{steady state}} = \phi A \omega_s \frac{(k_f^2 + \omega_s^2)^{1/2}}{[\omega_s^2 k_f^2 + (\omega_s^2 - k_f^2)^2]^{1/2}} \cos (\omega_s t + \psi)$$

Substitution of numerical values gives:

$$E_p^1 (t)\Big|_{max} = 0.00632 \quad \text{mrad}$$

With this information it is possible to compare errors in the various modes:

Autotrack: $\epsilon_{auto} = \sqrt{\epsilon_s^2 + \epsilon_R^2} = 0.163$ mrad

Program: $\epsilon_{prog} = \sqrt{\epsilon_s^2 + \epsilon_p^2} = 0.163$ mrad

Augmentation: $\epsilon_{aug} = \sqrt{\epsilon_s^2 + \epsilon_R^{1\,2} + \epsilon_p^{1\,2}} = 0.0553$ mrad

as is evident, tracking in the augmentation mode improves the accuracy by a factor of three.

It should be recalled, however, that the assumption has been made that program error and autotrack error are equal. For situations in which the program error is larger, due to severe misalignment of antenna boresite for example, the factor of improvement of the augmentation mode increases considerably.

Figure 4.3 shows the performance of the augmentation mode while tracking Nimbus IV at 136 MHz. Initially the antenna operates in the autotrack mode. Then the operator switches to program mode. Note the off-set in this mode which is due to antenna misalignments and predict errors. Finally the augmentation mode is selected and the error goes to essentially zero after one overshoot. While in program mode the operator could have introduced angular bias to reduce the off-set error, however this bias varies as the satellite pass progresses and is automatically achieved by selecting the augmentation mode.

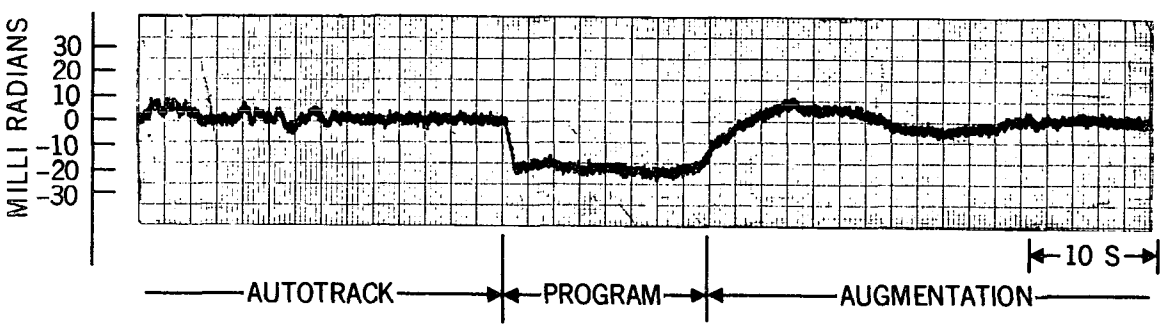

Figure 4-3. Performance of the Antuentation Mode

5. SUMMARY

The computer controlled antenna system has several advantages over the conventional system: reliability and consistency of operation, minimization of turn-around time between satellite passes, reduction on floor space requirements, fast identification of component or subsystem failures or misadjustments and in the case of new antenna procurements substantial savings on special equipment requirements. But above all there is one additional attribute and that is flexibility. Only software changes are required to change tracking algorithms, data to be monitored and to change the degree of automation desired.

All software programs have been written and checked using the 40 ft. antenna and the XDS Sigma 5 computer at NTTF. Test results have been extremely encouraging. Currently, an effort is in progress to duplicate this system using a smaller dedicated computer, a DEC PDP-11/20, in conjunction with the 40-ft. antenna. This new system will represent the final prototype for STDN antennas.

REFERENCES

1.1 George C. Winston: Antenna Control in Station Automation, GSFC Document X-525-67-496, December 1967.

2.1 Automatic Checkout and Adjustment Methods for the Servo and Control Systems of Large Steerable Antennas, Sylvania Electric Products, Inc., NASA Contract NAS5-10175, March 1967.

3.1 John J. Zarur: Antenna Control System, Wolf Research and Development Corp., NASA Contract NAS5-9756-192, February 1971.

3.2 J. T. Ton: Digital and Sampled-Data Control Systems, McGraw-Hill, 1959.

3.3 Daniel Tabak: Digitalization of Control Systems, Wolf Research and Development Corp., NASA Contract NAS5-9756-192.

3.4 M. Abramowitz, I. A. Stegun, Handbook of Mathematical Functions, National Bureau of Standards, June 1964.

4.1 H. Chestnut, R. W. Mayer, Servomechanisms and Regulating System Design, Volume II, John Wiley, Inc., 1955.

4.2 G. C. Newton, L. A. Gould, J. F. Kaiser, Analytical Design of Linear Feedback Control Systems, John Wiley, Inc., 1957.